Carrier-Induced Refractive Index Changes in InP-Based Circular Microresonators for Low-Voltage High-Speed Modulation

Thiruvikraman Sadagopan, *Student Member, IEEE*, Seung June Choi, *Member, IEEE*, Sang Jun Choi, Kostadin Djordjev, and P. Daniel Dapkus, *Fellow, IEEE*

***Abstract*—Optical InP-based microresonator modulators which achieve low-voltage high-bandwidth modulation are presented, where resonant wavelength tuning of a circular resonator by free carrier injection is used as the modulation mechanism. Since thermal effects in small resonant cavities and switching speed limitations posed by minority carrier lifetime are the primary concerns in such types of devices, ion bombardment in microtoroidal structures is used to increase the speed of response. The modulation speed is enhanced by an order of magnitude.**

***Index Terms*—High speed, ion bombardment, low voltage, microresonators, modulators, tunable filters, wavelength-division multiplexing.**

OPTICAL microresonators are compact and versatile elements capable of a variety of functionalities that are envisioned as useful elements in wavelength-division-multiplexing systems. Tunable filters, switchable optical ADD–DROP filters, lasers, and modulators have been proposed and the basic operational mechanisms demonstrated [1]–[4]. High quality factor (Q) active resonators utilizing free carrier injection (FCI) as a tuning/switching mechanism have been demonstrated [1]. In these devices, free carriers injected into the intrinsic region change the effective index of the whispering gallery modes (WGMs), and thus, blue-shift the resonant wavelengths in the spectral range of interest. Although other modulation mechanisms such as electroabsorption, depletion, and gain have been demonstrated [5], [6], we focus in this letter on the FCI mechanism as it is an attractive candidate to achieve low-voltage modulation in the InP-based material system.

A current limitation of these devices is their limited high-frequency response which is controlled by the minority carrier lifetime. Also, these devices exhibit thermal tuning under forward bias that limits their performance. In this letter, we demonstrate greater than an order of magnitude improvement in the operation bandwidth of FCI modulators through the use of proton implantation to reduce the minority carrier lifetime in these devices [7]. Low voltage operation is maintained by instituting fabrication approaches that improve the sensitivity of the ion implanted devices. We will also present a model of the tuning mechanism including the effects of both FCI and thermal effects that quantifies the speed–voltage swing tradeoff in these devices.

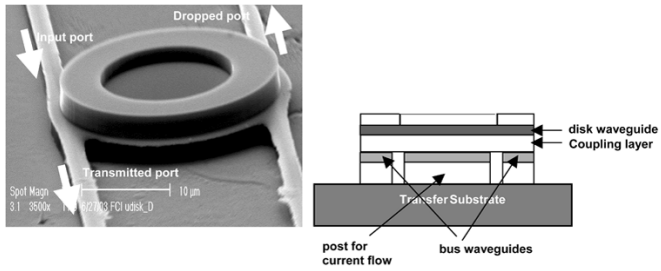

Fig. 1. SEM micrograph of a finished microtoroidal device is shown on the left. The device has a center void that is about 1.2 μm deep. The entire p region of the device is removed in the center to facilitate current flow only through the periphery of the device. The schematic cross section of the device shows the nature of the three-dimensional coupling.

The principle of operation of the FCI modulator involves the resonant transfer of optical energy between two waveguides at the resonance of a microresonator that couples them. An example of such a coupling structure is shown in Fig. 1. Modulation of light in the through port is accomplished by rapid tuning of the index of refraction and, thus, the resonant frequency of the microresonator by FCI.

The microresonator modulators in our study are fabricated with a combination of epitaxial growth and wafer bonding using a process that has been described in previous publications [1],[5], [8]. Some modifications have been introduced to maintain the small bias swing necessary to operate the modulator modified by the ion implantation process. Device fabrication starts with the growth of the epi-structure that contains the disk core with a sacrificial InGaAsP layer on top that will be removed after the ion implantation. This structure is bombarded with protons to achieve lifetime reduction. Protons with energy of 40 keV were chosen so as to cause maximum damage at the center of the disk waveguide core layer. After the ion implantation, the sacrificial layer is removed to provide a relatively defect free growth interface for the rest of the epitaxial structure. This consists of a 0.8-μm coupling layer and the bus waveguide core layer which is 0.4 μm thick followed by a 1-μm cladding layer for the bus waveguides. We believe that the regrowth procedure acts as an annealing mechanism that recovers the optical properties of the bombarded material. Hence, no significant change in the optical loss, which in turn affects the transmission properties (quality factors and contrast ratios) of the resonators, was observed. The processing of

Manuscript received July 14, 2004; revised September 20, 2004. This work was supported by Defense Advanced Research Projects Agency (DARPA) under the RFLIC program.

T. Sadagopan, S. J. Choi, S. J. Choi, and K. Djordjev are with the Department of Electrical Engineering-Electrophysics, University of Southern California, Los Angeles, CA 90089 USA.

P. D. Dapkus is with the Departments of Electrical Engineering and Materials Science, University of Southern California, Los Angeles, CA 90089-0243 USA (e-mail: dapkus@usc.edu).

Digital Object Identifier 10.1109/LPT.2004.839773

Report Documentation Page

Form Approved
OMB No. 0704-0188

1. REPORT DATE	2. REPORT TYPE	3. DATES COVERED
01 JUN 2005	**N/A**	**-**

4. TITLE AND SUBTITLE	5a. CONTRACT NUMBER
Carrier-Induced Refractive Index Changes in InP-Based Circular Microresonators for Low-Voltage High-Speed Modulation	5b. GRANT NUMBER
	5c. PROGRAM ELEMENT NUMBER
6. AUTHOR(S)	5d. PROJECT NUMBER
	5e. TASK NUMBER
	5f. WORK UNIT NUMBER
7. PERFORMING ORGANIZATION NAME(S) AND ADDRESS(ES) **Department of Electrical Engineering-Electrophysics, University of Southern California, Los Angeles, CA 90089 USA**	8. PERFORMING ORGANIZATION REPORT NUMBER
9. SPONSORING/MONITORING AGENCY NAME(S) AND ADDRESS(ES)	10. SPONSOR/MONITOR'S ACRONYM(S)
	11. SPONSOR/MONITOR'S REPORT NUMBER(S)

12. DISTRIBUTION/AVAILABILITY STATEMENT
Approved for public release, distribution unlimited

13. SUPPLEMENTARY NOTES
See also ADM001923.

14. ABSTRACT

15. SUBJECT TERMS

16. SECURITY CLASSIFICATION OF:			17. LIMITATION OF ABSTRACT	18. NUMBER OF PAGES	19a. NAME OF RESPONSIBLE PERSON
a. REPORT	b. ABSTRACT	c. THIS PAGE			
unclassified	**unclassified**	**unclassified**	**UU**	**3**	

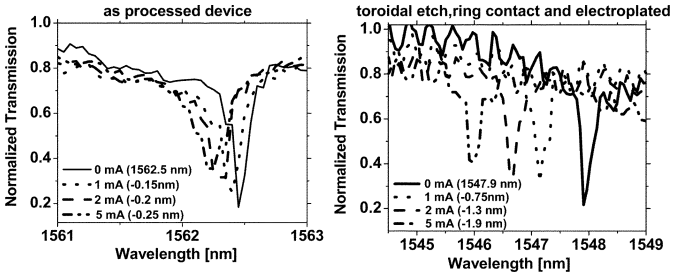

Fig. 2. Comparison of tuning capabilities between a 12-μm microdisk and microtoroidal device. The device on the right is a microtoroidal device that has a center void that is 8.5 μm in radius. The tuning capability has increased from 0.15 to 0.75 nm/mA.

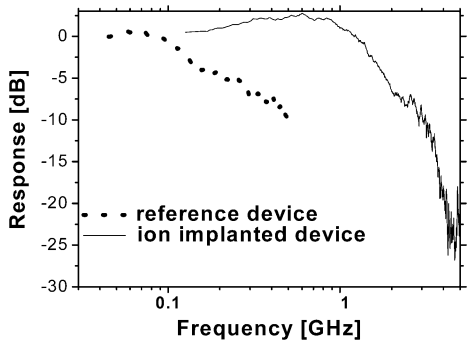

Fig. 3. Frequency response of an FCI microtoroidal device that was proton implanted at 40 keV at a dosage of $10^{14}/\text{cm}^2$. The device exhibits a 3-dB bandwidth of about 1.5 GHz. In comparison, the reference device exhibited a 3-dB bandwidth close to 130 MHz. The devices were dc-biased with current = 1 mA.

these devices including patterning the bus waveguides, wafer bonding, etching of the disk mesas, polyimide planarization, and metallization is described in an earlier letter [8]. An additional etching step chosen only to penetrate the top p-layer is included in our processing to define a center void in these devices. This reduces the active area and increases the sensitivity of the devices to current bias [9] since current flowing through the center of the device does not interact with the WGM in the microdisk. A schematic and a scanning electron micrograph (SEM) of the microtoroidal device are shown in Fig. 1. The entire device structure is planarized using polyimide and contact pads are patterned to allow probing and wire bonding. Thick gold is electroplated on the top contact to facilitate bonding and to act as a conductive heat path from the top of the device.

The transmission properties of our resonators are measured with a tunable continous-wave laser diode. The light is coupled into the input bus waveguide using a lensed fiber and coupled out of the throughput using a microscope objective and free space alignment. For high-speed measurements, a network analyzer is used with the samples mounted on a high-speed submount. A comparison of a reference (unimplanted) and an ion implanted sample without the center void showed that the sensitivity in the latter case was reduced from 0.7 to 0.15 nm/mA. This loss of sensitivity is recovered by etching the center void. Fig. 2 shows the normalized transmission characteristics of 12-μm radii FCI microdisk modulators that were implanted with 40-keV protons at a dosage of $10^{14}/\text{cm}^2$. The device on the left is a microdisk device. The one on the right is a 12-μm microtoroidal device complete with an 8.5-μm center void. The small wiggles that we see in the transmission characteristics are Fabry–Pérot resonances due to imperfect antireflection coating at the facets of the device. We see that there is considerable improvement in tuning of the microtoroidal structure as compared to the microdisk. Fig. 3 shows the high-frequency response of this device and an unimplanted one from similar materials. The measured device has a 3-dB bandwidth of 1.5 GHz. In comparison, the reference shows a bandwidth of around 150 MHz. Switching near current turn on requires 300 μA (0.3 V) to switch the device similar to that described previously in unimplanted microdisk switches [1]. Higher implantation doses and narrower toroidal rings will improve the frequency bandwidth in these devices while maintaining the very low current swing that is achieved in the present devices.

Since the use of ion implantation to increase the operational bandwidth of the device also increases the current density swing required to achieve a given resonance tuning, there is an inherent speed–sensitivity tradeoff operative in these devices. Because heating produces a resonance tuning in the opposite direction to the FCI, there will be a limit to the modulation speed that one can achieve in these devices. To understand these limits, we have developed a model that includes the current tuning from FCI and the accompanying heating effects owing to current flow. The operation of an FCI modulator primarily relies on the refractive index changes that are caused by the free carriers injected into an undoped GaInAsP waveguide core [10] that causes a blue-shift in the resonant wavelength of the microresonator. The carrier density and, hence, the refractive index are functions of the current are described by the following equations:

$$\frac{\eta_i \times I}{q\nu} = \frac{N}{\tau} = A \times N + B \times N^2 + C \times N^3 \qquad (1)$$

and

$$\Delta n = -aN + n(T) - n(T_{\text{HS}}) \qquad (2)$$

where τ denotes the carrier lifetime, n denotes the refractive index, N is the carrier density, I is the current, ν is the volume of the microcavity, η_i is the internal efficiency, T is the temperature of the device, T_{HS} is the temperature of the heat sink, and q is the electronic charge. A, B, and C represent the nonradiative, radiative, and Auger recombination coefficients, respectively. $a = 1.1 \times 10^{-20}$ is a constant that depends on the electron effective mass, the photon energy, and the refractive index [13]. The temperature of the heat sink is taken to 300 K.

As seen from [11, eq. (1)], a large part of the speed–sensitivity tradeoff arises because the lifetime reduction requires more current to be injected to achieve the same carrier density. This can be balanced by reducing the active volume of the device. This motivated our additional etch step to form a microtoroid, as shown in Fig. 1.

The first term in (2) quantifies the effect of free carriers on the refractive index of the material [12] that is mainly intended in FCI tuning. The next two terms describe the temperature-induced change in index that is an unintended consequence of the current flow in the device. This is primarily affected by the physical geometry and the nature of materials used for the resonator.

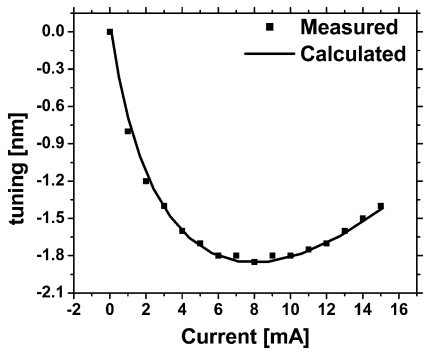

Fig. 4. Calculated and measured tuning curves for a 12-μm microdisk modulator.

The effect of temperature is calculated by assuming that the temperature of the tuning region and the cladding layer immediately around it is uniform and that all the power in the structure is dissipated there [12]. The temperature is then given by

$$T = T_{\rm HS} + R_{\rm th} IV \tag{3}$$

where $T_{\rm HS}$ is the temperature of the heat sink, $R_{\rm th}$ is the thermal resistance of the device, I is the current, and V is the voltage across the device. The thermal resistance is used as a fitting parameter. The refractive index change due to temperature is computed for InGaAsP material using the model by Adachi [13].

The temperature dependence of the index occurs through two parameters E_g, the energy bandgap, and $\varepsilon_{\rm inf}$, the high frequency dielectric constant. The temperature dependence of E_g and $\varepsilon_{\rm inf}$ near 300 K is obtained from [14]–[16].

We also calculate the change in the refractive index of the device as the current flows and heats up the device. As the temperature increases, the red-shift in wavelength resulting from heating competes with the blue-shift resulting from the carrier injection. The effect of temperature computed using this model is in tune with the 0.1-nm/°C shift generally observed in InP. The modal index change is then calculated using the conformal transformation approach for a microdisk [17].

Fig. 4 shows the calculated and measured tuning curves for a 12-μm FCI microdisk.

We see that the calculation is in good agreement with the measured data. The value of thermal resistance of the device used in the calculation was 4500 K/W. This value is close to those reported by other workers for microdisk resonators [18]. Based on these calculations, we expect that the lower limit on the bandwidth of this device design can be increased to around 10 GHz with further implantation reduction of the minority carrier lifetime and by using a smaller ring design to improve current sensitivity. The maximum bandwidth occurs when the heating-induced change of the index balances that of the FCI. The time constants of these two effects are dramatically different and the important issue is the differential tuning at the operational speed. Thus, the limit estimated in this way is a lower bound on the bandwidth. The temperature effects, however, cause a slow change in the background of the response. This needs to be addressed by using additional means to stabilize the device and, hence, improve performance.

In conclusion, we have analyzed the FCI mechanism in microdisk devices. An analysis including the effects of temperature was presented that accurately predicts the steady state tuning characteristics of the resonators. The possibility of achieving higher modulation bandwidths by reducing the carrier lifetime through ion implantation was also demonstrated. The analysis shows that higher dose ion implantation will lead to further improvements in the bandwidths in these devices. The sensitivity of the devices was maintained by using a microtoroidal design to prevent current flow at the center of the circular microresonators. In this manner, modulators that operate with low voltages and have 3-dB bandwidths close to 1.5 GHz were demonstrated. Analysis suggests that bandwidths higher than 10 GHz can be achieved with further device improvements.

REFERENCES

[1] K. D. Djordjev, S. J. Choi, S. J. Choi, and P. D. Dapkus, "Microdisk tunable resonant filters and switches," *IEEE Photon. Technol. Lett.*, vol. 14, no. 6, pp. 828–830, Jun. 2002.

[2] K. Djordjev *et al.*, "Active semiconductor microdisk devices," *J. Lightw. Technol.*, vol. 20, no. 1, pp. 105–113, Jan. 2002.

[3] K. Djordjev, S. J. Choi, S. J. Choi, and P. D. Dapkus, "Vertically coupled InP microdisk devices with electroabsorption active regions," *IEEE Photon. Technol. Lett.*, vol. 14, no. 8, pp. 1115–1117, Aug. 2002.

[4] ——, "Gain trimming of the resonant characteristics in vertically coupled InP microdisk switches," *Appl. Phys. Lett.*, vol. 80, no. 19, pp. 3467–3469, May 2002.

[5] K. D. Djordjev, "Active microdisk resonant devices and semiconductor optical equalizers as building blocks for future photonic circuitry," Ph.D. dissertation, Univ. Southern California, 2002.

[6] T. C. Huang, T. Hausken, K. Lee, N. Dagli, L. A. Coldren, and D. R. Myers, "Depletion edge translation waveguide crossing optical switch," *IEEE Photon. Technol. Lett.*, vol. 1, no. 7, pp. 168–170, Jul. 1989.

[7] K. F. Lamprecht, S. Juen, L. Palmetshofer, and R. A. Hopfel, "Ultrashort carrier lifetimes in $H+$ implanted InP," *Appl. Phys. Lett.*, vol. 59, no. 8, pp. 926–928, Aug. 1991.

[8] S. J. Choi, K. Djordjev, S. J. Choi, and P. D. Dapkus, "CH4-Based dry etching of high Q InP microdisks," *J. Vac. Sci. Technol. B*, vol. 20, pp. 301–305, Jan. 2002.

[9] T. Sadagopan, S. J. Choi, S. J. Choi, P. D. Dapkus, and A. E. Bond, "High-Speed, low-voltage modulation in circular WGM microresonators," in *Proc. IEEE LEOS Summer Topical Meetings*, Jun. 2004, pp. MC 2–3.

[10] B. R. Bennett, R. A. Soref, and J. A. D. Alamo, "Carrier-Induced change in refractive index of GaAs, InP and InGaAsP," *IEEE J. Quantum Electron.*, vol. 26, no. 1, pp. 113–122, Jan. 1990.

[11] L. A. Coldren and S. W. Corzine, *Diode Lasers and Photonic Integrated Circuits*, K. Chang, Ed. New York: Wiley, 1995.

[12] J. P. Weber, "Optimization of the carrier-Induced effective index change in InGaAsP waveguides- application to tunable bragg filters," *IEEE J. Quantum Electron.*, vol. 30, pp. 1801–1816, Aug. 1994.

[13] S. Adachi, *Physical Properties of III–V Semiconductor Compounds*. New York: Wiley, 1992.

[14] G. Schraud, G. Muller, L. Stoll, and U. Wolff, "Simple measurement of carrier-Induced refractive-index change in InGaAsP PIN ridge waveguide structures," *Electron. Lett.*, vol. 27, no. 4, pp. 297–298, Feb. 1991.

[15] G. P. Agrawal and N. K. Dutta, *Long Wavelength Semiconductor Lasers*. New York: Van Nostrand, 1986.

[16] A. Katz, Ed., *Indium Phosphide and Related Materials: Processing, Technology and Devices*. Boston, MA: Artech House, 1992.

[17] M. K. Chin and S. T. Ho, "Design and modeling of waveguide-coupled single-mode microring resonators," *J. Lightw. Technol.*, vol. 16, no. 8, pp. 1433–1446, Aug. 1998.

[18] R. Ushigome, M. Fujita, A. Sakai, T. Baba, and Y. Kokobun, "GaInAsP microdisk injection laser with benzocyclobutene polymer cladding and its athermal effect," *Jpn. J. Appl. Phys.*, vol. 41, pp. 364–6369, Nov. 2002.